Cognitive Small Cell Networks: Energy Efficiency and Trade-Offs

Matthias Wildemeersch, *Student Member, IEEE,* Tony Q. S. Quek, *Senior Member, IEEE,* Cornelis H. Slump, *Member, IEEE,* and Alberto Rabbachin, *Member, IEEE*

***Abstract*—Heterogeneous networks using a mix of macrocells and small cells are foreseen as one of the solutions to meet the ever increasing mobile traffic demand. Nevertheless, a massive deployment of small cell access points (SAPs) leads also to a considerable increase in energy consumption. Spurred by growing environmental awareness and the high price of energy, it is crucial to design energy efficient wireless systems for both macrocells and small cells. In this work, we evaluate a distributed sleep-mode strategy for cognitive SAPs and we analyze the trade-off between traffic offloading from the macrocell and the energy consumption of the small cells. Using tools from stochastic geometry, we define the user discovery performance of the SAP and derive the uplink capacity of the small cells located in the Voronoi cell of a macrocell base station, accounting for the uncertainties associated with random position, density, user activity, propagation channel, network interference generated by uncoordinated activity, and the sensing scheme. In addition, we define a fundamental limit on the interference density that allows robust detection and we elucidate the relation between energy efficiency and sensing time using large deviations theory. Through the formulation of several optimization problems, we propose a framework that yields design guidelines for energy efficient small cell networks.**

***Index Terms*—Small cell, cognitive radio, green communications, stochastic geometry, energy efficiency.**

I. Introduction

OVER the last years mobile data traffic has risen exponentially and along with this accruing mobile data demand, energy consumption has increased considerably [1]–[3]. Driven by growing environmental awareness and increasing electrical cost relative to the operation of mobile base stations (MBSs), green wireless communications has become an active field of research that tries to unite the opposing needs of growing mobile data activity and energy efficiency [4]–[6].

Manuscript received August 10, 2012; revised February 13 and May 13, 2013. The editor coordinating the review of this paper and approving it for publication was H. Yanikomeroglu.

The material in this paper has been presented in part at the IEEE Wireless Communications and Networking Conference (WCNC), Shanghai, China, April 2013, and at the IEEE International Conference on Communications (ICC), Budapest, Hungary, June 2013.

M. Wildemeersch is with the Signals and Systems Group, University of Twente, the Netherlands, and the Institute for Infocomm Research, A*STAR, Singapore (e-mail: stuwma@i2r.a-star.edu.sg).

T. Q. S. Quek is with the Singapore University of Technology and Design, and the Institute for Infocomm Research (e-mail: qsquek@ieee.org).

C. H. Slump is with the Signals and Systems Group, University of Twente, Drienerlolaan 5, 7500 AE Enschede, the Netherlands (e-mail: C.H.Slump@utwente.nl).

A. Rabbachin is with the Laboratory for Information and Decision Systems (LIDS), Massachusetts Institute of Technology, 77 Massachusetts Avenue, Cambridge, MA 02139 USA (e-mail: rabalb@mit.edu).

Digital Object Identifier 10.1109/TCOMM.2013.072213.120588

Conventional cellular networks based on the careful deployment of MBSs suffer from poor signal quality for indoor and cell edge users. Furthermore, the explosive surge in mobile data traffic accelerates the need for novel cellular architectures to meet such demands [3]. The LTE-Advanced or beyond standards propose heterogeneous networks (HetNet's) that consist of a macrocell network overlayed by small cells. The macro-tier guarantees the coverage, while the overlay network is a means to offload the data traffic from the macrocell network and to satisfy the local capacity demand. The small cells in this two-tier architecture can be micro-cells, pico-cells or femto-cells, where the distinction between the different types of small cells can be found in the size of the cells and the capability of auto-configuration and auto-optimization. Small cells can extend the network coverage and the reduced cell size leads to higher spatial frequency reuse and increased network capacity.

Although the introduction of heterogeneous networks can resolve the capacity demand issue [7], [8], the overall energy consumption is significantly increased by the installation of these additional base stations. Motivated by the high traffic demand fluctuations over space, time, and frequency, sleep mode techniques are a promising strategy to overcome this problem. For wireless sensor networks, the energy conservation by sleeping techniques for wireless devices running on battery power has been studied in [9]. The IEEE 802.16e and LTE standards support sleep mode strategies for mobile terminals and the trade-off between energy efficiency and response delay has been analyzed in [10]. Only some recent work is dedicated to sleep mode techniques for small cell access points (SAPs). In [11], the authors conclude that sleep mode operation is effective when the cell size is small and for light traffic conditions. Different sleep mode strategies for SAPs are introduced in [12], such that the wake-up mechanism can be driven by the SAP, the core network or the user equipment (UE). For WiFi access points, the UE driven approach has been studied in [13], but the reverse beaconing adds complexity to the hardware and assumes knowledge about the signal structure. In [14], the overall HetNet energy consumption is minimized based on sleep mode techniques for network-operated femtocells. This centralized sleep and wake-up mechanism assumes traffic load and user localization awareness, and increases the signaling overhead. Therefore, it is attractive to investigate distributed sleep mode strategies, which do not involve an augmented UE complexity and require neither signaling nor user localization awareness.

To allow a distributed decision approach, the SAP needs cognitive capabilities to sense when a small cell user is active within the SAP coverage [12]. In future heterogeneous networks, cognitive capabilities will become essential not only for the energy efficient operation of the small cell tier, but also to overcome coexistence issues in multi-tier networks. Specifically, spectrum or carrier sensing by the cognitive SAPs enable interference avoidance and efficient spectrum allocation [15]. Hence, cognitive small cells allow the deployment of energy efficient and spectral efficient heterogeneous networks. Many ideas can be borrowed from the field of cognitive radio (CR). For cognitive radio networks (CRN), the trade-off between protection of the primary users (PU) and the throughput of the secondary users (SU) has been addressed in [16]–[18]. For SAP sleep mode techniques, this corresponds to the trade-off between traffic offload by means of a high detection probability and energy consumption, proportional to the false alarm rate. Although spectrum sensing and cognitive radio are intensely studied, there are still many issues that need to be addressed [19]–[22]. For instance, the cognitive capabilities are usually assessed for a deterministic (worst case) user location, while a random position of the user is of interest to determine energy consumption. The capacity and energy efficiency of base stations in heterogeneous networks has been studied in [23], but the impact of aggregate interference in dense network deployments has typically been neglected. Recent results show that it is fundamental to consider aggregate interference to accurately define the network performance [24]–[26].

In this work, we investigate how SAPs can be used to offload the traffic from the macrocell network and how they can exploit their sensing capabilities to enhance the energy efficiency. Specifically, these energy efficient SAPs can save power by entering into sleep mode when they are not serving any active small cell users. Considering open access control, the SAPs need to sense the transmissions from a macrocell user to an MBS, and switch on the pilot transmissions when user activity is detected within the SAP coverage. Due to the simplicity of passive sensing, we assume that all SAPs perform energy detection at the expense of being sensitive to noise and interference uncertainties. Furthermore, the transmissions from the macrocell user can be bursty, making the duty cycle of the sleeping mode at each SAP difficult to design to ensure a low probability of miss detection. Since the analysis of a deterministic (e.g. worst case) user location does not provide guidance for the definition of the SAP energy consumption, it is crucial to evaluate the typical user case, that is, to consider a user with random location within the SAP coverage. Specifically, the main contributions of this work are listed as follows:

- We formulate an average network energy consumption model for the cognitive SAPs that are located within the Voronoi cell of an MBS accounting for the base station and user densities, detection performance, the sensing strategy, bursty macrocell user activity, and uncoordinated network interference uncertainties.
- We present a unified analytical framework that models the performance of passive sensing for a typical user within the SAP coverage, including the effects of propagation channel and aggregate network interference.
- We derive tractable expressions of the aggregate throughput and capacity that can be offloaded by the small cells within an the MBS Voronoi cell. This allows us to formulate the trade-off between energy consumption and throughput/capacity as a set of optimization problems.
- We define the interference wall, beyond which the target probability of detection and false alarm can not be obtained no matter how long the sensing time. This is a fundamental limit of the detection robustness, which confines the region of interferer densities enabling an energy efficient SAP design.
- Using techniques from large deviations theory, we determine how fast the false alarm rate converges to a stationary value as a function of the interferer density. The obtained rate function gives insight into how the detection performance affects the small cell energy consumption and traffic offload.

The remainder of the paper is structured as follows. In Section II, the system model is introduced. In Section III, the energy consumption model and the sensing performance of the SAP are discussed. The traffic that can be offloaded from the macrocell is characterized in Section IV. In Section V, the trade-off between traffic offload and energy consumption is discussed by means of several optimization problems. The limits of detection robustness and the implications on the energy efficiency are discussed in Section VI. Numerical results are shown in Section VII and conclusions are drawn in Section VIII.

II. System Model

A. Network topology

We consider a cellular network model that consists of a first tier of MBSs distributed according to a homogeneous Poisson point process (PPP) Θ with density λ_{m}, overlayed with a network of SAPs distributed according to a PPP Φ with density λ_{s}, where usually $\lambda_{\mathrm{s}} > \lambda_{\mathrm{m}}$. Modeling the locations of SAPs and the more regular MBSs by means of homogeneous PPPs is extensively discussed in literature and has been validated by numerical analysis and compared with actual base station deployments [27]. Moreover, recently theoretical evidence has been given for the accuracy of the PPP model [28]. The set of macrocells is known as the Poisson-Voronoi tessellation of $\mathbb{R}^2$ with respect to Θ. The Voronoi cell C_j corresponding to an MBS $x_{j,\mathrm{m}}$ consists of those points in $\mathbb{R}^2$ which are closer to $x_{j,\mathrm{m}}$ than to any other MBS and is defined as $C_j = \{y \in \mathbb{R}^2 \mid \|y - x_{j,\mathrm{m}}\| \leq \|y - x_{i,\mathrm{m}}\|, x_{i,\mathrm{m}} \in \Theta \backslash \{x_{j,\mathrm{m}}\}\}$. The SAPs that belong to C_j form the aggregate $A_j = \cup\{x_{i,\mathrm{s}} \mid x_{i,\mathrm{s}} \in \Phi \cap C_j\}$, and applying Campbell's theorem the mean number of SAPs within an MBS Voronoi cell is given by $\lambda_{\mathrm{s}}/\lambda_{\mathrm{m}}$ [29]. The mobile users are scattered over $\mathbb{R}^2$ according to a PPP Ψ with density λ_{u}.[1] We consider universal spectrum allocation where both tiers can access the full spectrum and orthogonal frequency-division multiple access (OFDMA) or time-division multiple access (TDMA) as multiple access technique.[2] The SAPs operate in open access

[1]Note that Θ, Φ, and Ψ are independent point processes.

[2]The analysis can be extended to orthogonal spectrum allocation and affects the interferer densities, which is important for the performance detection and the offload analysis discussed in Section III-B and IV, respectively.

(OA) mode and are accessible for all users registered with the operator of the SAP. In order to enable a distributed sleep/wake-up scheme, the SAPs are foreseen of cognitive capabilities. When an SAP does not serve an active user call, it goes into sleep mode and senses periodically the macrocell uplink channel to detect user activity. The SAP applies passive sensing by means of an energy detector (ED) for reasons of low complexity and low power consumption [30]. The ED detection performance compared with other detection schemes has been studied exhaustively in literature [31], [32]. We limit our analysis to the ED since this scheme provides a lower detection bound. Once the SAP detects an active user in the macrocell uplink band within its coverage, the SAP switches on and starts the transmission of pilot signals. Subsequently, the UE reports the presence of the SAP to the MBS and the UE is handed over to the SAP. We assume that the uplink transmission power of the UE during the sensing period is constant and that after handover to the SAP, the UE adopts a lower and constant transmission power. It is well known that the ED has no capabilities to differentiate between the signal of interest (SoI) and interference or noise [30]. The measurements of the SAP under realistic conditions are corrupted by network interference, which can originate from macrocell users outside the SAP coverage, macrocell users within the SAP coverage that are not registered with the SAP operator, small cell users, cognitive devices using the same uplink band, and spurious emissions. As a result, we consider the case of the interfering nodes spatially distributed over the entire plane according to a homogeneous PPP Ω with density λ.[3] For a homogeneous PPP, the probability that k nodes reside within a region $\mathcal{R}$ depends on the density λ and the area $A_{\mathcal{R}}$ of the region $\mathcal{R}$, and can be expressed as [33]

$$\mathbb{P}[k \in \mathcal{R}] = \frac{(\lambda A_{\mathcal{R}})^k}{k!} e^{-\lambda A_{\mathcal{R}}}, \quad k = 0, 1, 2, ... \qquad (1)$$

The spatial model consisting of a macrocell network overlayed with multiple small cells is illustrated in Fig. 1.

B. Activity model

We define the activity of the UEs and SAPs using a time-slotted model as depicted in Fig. 2. Assuming a fixed slot duration T, the SAP senses the channel over a sensing time τ_{s} and is in active mode over $T-\tau_{\mathrm{s}}$ when an active mobile user is detected[4]. Both the UE and the interfering nodes are assumed to have a bursty traffic mainly due to the mobility of the nodes, the switching between on and off states, and the switching between carriers in a multi-carrier system. Thus, the activity of an SAP, a UE and the interfering nodes in a given slot can be modeled as mutually independent Bernouilli processes with success probabilities p_{s}, p_{u}, and p_{I}, respectively. Moreover, the activity of the SAP, the UE, and the interfering nodes is assured to be independent across different slots. By the colouring theorem of PPPs, the active nodes that contribute to the interference form a PPP with density $p_{\mathrm{I}}\lambda$ [33]. We will further refer to p_{s} as the sensing probability.

[3]Note that the model allows to include the presence of groups of interferers with different transmission power. The superposition of PPP's with densities λ_1, λ_2, ... results in a PPP with density equal to a weighted sum of the densities, where the weighting factor depends on the transmission power P_i of the different PPPs and is given by $\lambda = \sum_i \lambda_i (P_i/P_{\mathrm{u}})^{2/\nu}$, with P_{u} the transmit power of the UE, and ν the path loss exponent.

[4]Active mode consists of transmitting pilot signals, receiving signals, and signal processing. Note that we neglect the time related to the handover process for simplicity.

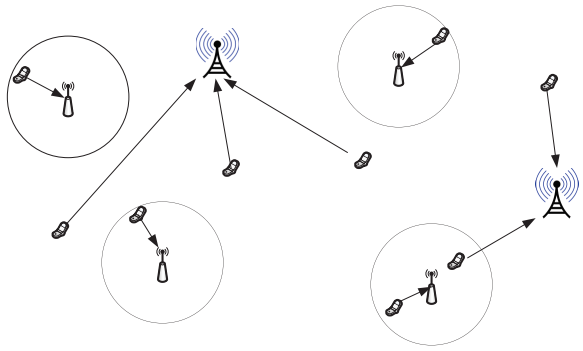

Fig. 1. Spatial distribution of the MBSs, SAPs, and the UEs.

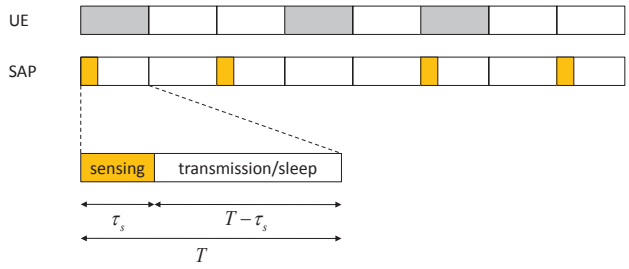

Fig. 2. Time slotted model, representing the activity of UE and the SAP over time.

III. Cognitive SAP

In the following, we provide the average network energy consumption model for the SAPs and we characterize the relationship between the energy consumption and the detection performance of the cognitive SAP. The presented analysis is generic and accommodates for random locations of both the UE and the interfering nodes.

A. Energy consumption model

Three main contributions to the power consumption of cognitive SAPs can be identified: the power related to the circuit synchronization Ξ_c, the sensing power Ξ_{s}, and the processing power Ξ_t during active mode [34]. We consider the circuit synchronization is active over the entire time slot. The SAP senses the uplink channel according to a sensing scheme and the corresponding energy consumption is proportional to the sensing time. The UE signal detection is a binary hypothesis test problem. In the presence of a UE signal (hypothesis $\mathcal{H}_1$), the SAP starts the pilot transmissions when it senses the uplink channel and correctly detects the user activity. In the absence of the UE signal (hypothesis $\mathcal{H}_0$), the SAP starts the pilot transmissions when it incorrectly detects the presence of a user. The probability that there resides at least one active UE within the coverage of a typical SAP is

$$\psi_{V_{\mathrm{ED}}|\mathcal{H}_1}(j\omega) = \frac{1}{(1-2j\omega\sigma_W^2)^{N/2}}\left[1 - {}_2F_1\left(1, \frac{2}{\nu}; 1+\frac{2}{\nu}; \frac{R^\nu(1-2j\omega\sigma_W^2)}{j\omega P_{\mathrm{u}}}\right)\right] \times \exp\left\{-2^{2/\nu}\gamma\cos(\pi/\nu)\left|\frac{j\omega}{1-2j\omega\sigma_W^2}\right|^{2/\nu}\left[1-\mathrm{sign}\left(\frac{j\omega}{1-2j\omega\sigma_W^2}\right)\tan(\pi/\nu)\right]\right\} \quad (10)$$

given by $p_{\mathrm{UE}} = 1-\exp(-p_{\mathrm{u}}\lambda_{\mathrm{u}}\pi R^2)$. Therefore, the expected SAP energy consumption per cell can be modeled as

$$E_{\mathrm{tot}} = \frac{\lambda_{\mathrm{s}}}{\lambda_{\mathrm{m}}}[\Xi_c T + p_{\mathrm{UE}}\{p_{\mathrm{s}}[\Xi_{\mathrm{s}}\tau_{\mathrm{s}} + \mathbb{P}_{\mathrm{d}}\Xi_t(T-\tau_{\mathrm{s}})]\} + (1-p_{\mathrm{UE}})\{p_{\mathrm{s}}[\Xi_{\mathrm{s}}\tau_{\mathrm{s}} + \mathbb{P}_{\mathrm{fa}}\Xi_t(T-\tau_{\mathrm{s}})]\}] \quad (2)$$

where $\mathbb{P}_{\mathrm{d}}$ and $\mathbb{P}_{\mathrm{fa}}$ are the probability of user activity detection and false alarm, respectively.

B. Non-coherent detection performance

Since the presence of multiple simultaneous UE transmissions in the macrocell uplink band eases the detection process, we consider the more challenging scenario with a single UE within the coverage of an SAP to define the detection performance. At the cognitive SAP, the received signal can be written as

$$\begin{aligned}\mathcal{H}_0 &: r(t) = n(t) + i(t)\\ \mathcal{H}_1 &: r(t) = \frac{h(t)}{r_{\mathrm{f}}^{\nu/2}}s(t) + n(t) + i(t)\end{aligned} \quad (3)$$

where $s(t)$, $n(t)$, and $i(t)$ represent the SoI, the additive white Gaussian noise and the aggregate network interference, respectively. The impulse response of the flat fading channel between the UE and SAP is represented by $h(t)$, r_{f} is the distance between the UE and the SAP, and ν is the power path loss exponent. To facilitate the analysis, we consider that the typical SAP is at the origin of the Euclidean plane and the coverage of the SAP is a circular area around the origin with radius R. The energy of the SoI at the SAP can be written as $P_{\mathrm{u}} r_{\mathrm{f}}^{-\nu} h^2$, where P_{u} is the transmit power of the UE. We assume there is no power control in the macrocell network, and therefore, P_{u} is independent of the distance between the UE and the MBS.[5] The noise term has a zero-mean Gaussian distribution $n(t) \sim \mathcal{N}(0, \sigma_n^2)$. The interfering nodes consist of macrocell users, small cell users belonging to other SAPs, or (cognitive) devices which are active on the same band. Therefore, the aggregate network interference measured at the SAP can be written as

$$i(t) = \mathfrak{Re}\left\{\sum_{l=1}^{\infty} i_l(t)\right\} = \mathfrak{Re}\left\{\sum_{l=1}^{\infty}\frac{h_l \mathbf{X}_l^{\mathrm{i}}}{r_{\mathrm{f},l}^{\nu/2}}\right\} \quad (4)$$

where we model the lth interferer amplitude $\mathbf{X}_l^{\mathrm{i}} = X_{l,1}^{\mathrm{i}} + jX_{l,2}^{\mathrm{i}}$ as a zero-mean complex random variable (r.v.). Note that the r.v.'s $\mathbf{X}_l^{\mathrm{i}}$ are circular symmetric, and independent and identically distributed (i.i.d.) in l since the interferers transmit independently. Therefore, with the interfering nodes scattered over $\mathbb{R}^2$ according to a PPP, the aggregate network interference follows a symmetric stable distribution [35], [36]

$$i \sim \mathcal{S}(\alpha = 4/\nu, \beta = 0, \gamma = \pi\lambda C_{4/\nu}^{-1}\mathbb{E}[|h_l X_{l,p}^{\mathrm{i}}|^{4/\nu}]) \quad (5)$$

with C_x defined as

$$C_x \triangleq \begin{cases}\frac{(1-x)}{\Gamma(2-x)\cos(\pi x/2)}, & x \neq 1,\\ \frac{2}{\pi}, & x = 1.\end{cases} \quad (6)$$

The decision variable V determines the presence or absence of the SoI. For the ED, V is defined as

$$V = \frac{1}{\tau_{\mathrm{s}}}\int_0^{\tau_{\mathrm{s}}}\left(\frac{h(t)}{r_{\mathrm{f}}^{\nu/2}}s(t) + n(t) + i(t)\right)^2 dt. \quad (7)$$

After sampling and considering block fading, the decision variable can be expressed as

$$V_{\mathrm{ED}} = \frac{1}{N}\sum_{k=1}^{N} r^2[k] = \frac{1}{N}\sum_{k=1}^{N}\left(\frac{h}{r_{\mathrm{f}}^{\nu/2}}s[k] + i[k] + n[k]\right)^2 \quad (8)$$

where $N = \lfloor \tau_{\mathrm{s}} f_{\mathrm{s}} \rfloor$ with f_{s} the sampling frequency equal to the Nyquist rate[6]. The probability of detection is defined as the probability that V_{ED} surpasses the threshold ζ in the presence of the SoI and is given by $\mathbb{P}_{\mathrm{d}} = \mathbb{P}[V_{\mathrm{ED}} > \zeta|\mathcal{H}_1]$. The probability of false alarm is defined as the probability that V_{ED} surpasses the threshold in absence of the SoI and is given by $\mathbb{P}_{\mathrm{fa}} = \mathbb{P}[V_{\mathrm{ED}} > \zeta|\mathcal{H}_0]$. To calculate $\mathbb{P}_{\mathrm{d}}$ and $\mathbb{P}_{\mathrm{fa}}$, we propose a generic approach based on the characteristic function (CF) of the decision variable. Using the inversion theorem, the probability that the decision variable surpasses the threshold can be found as

$$\mathbb{P}[V_{\mathrm{ED}} > \zeta] = \frac{1}{2} - \frac{1}{2\pi}\int_0^{\infty}\mathfrak{Re}\left\{\frac{\psi_{V_{\mathrm{ED}}}(-j\omega)e^{j\omega\zeta} - \psi_{V_{\mathrm{ED}}}(j\omega)e^{-j\omega\zeta}}{j\omega}\right\}d\omega \quad (9)$$

where $\psi_{V_{\mathrm{ED}}}$ represents the CF of V_{ED}. Under $\mathcal{H}_1$, $\psi_{V_{\mathrm{ED}}}$ is provided in the following theorem for a typical user, i.e. a user with random location within the small cell coverage.

Theorem 1: In the presence of Rayleigh block fading, the CF of the ED decision variable for a typical user in the presence of interference uncertainties is given by (10) where ${}_2F_1(.)$ is the Gaussian hypergeometric function.

Proof: See Appendix A. □

For the calculation of $\mathbb{P}_{\mathrm{fa}}$ in the presence of aggregate interference, we apply the same methodology as in Appendix A, yet in absence of the SoI. The CF of the decision variable under $\mathcal{H}_0$ can be expressed as (11) at the top of the next page, and $\mathbb{P}_{\mathrm{fa}}$ can be obtained applying the inversion theorem.

[5]Since the users that benefit most from the deployment of small cells are located far away from the MBS, our model holds for the cell edge users who transmit at maximum power.

[6]For simplicity, we assume $N = \tau_{\mathrm{s}} f_{\mathrm{s}}$

$$\psi_{V_{\mathrm{ED}}|\mathcal{H}_0}(j\omega) = \frac{1}{\left(1-2j\omega\sigma_W^2\right)^{N/2}} \times \exp\left\{-2^{2/\nu}\gamma\cos(\pi/\nu)\left|\frac{j\omega}{1-2j\omega\sigma_W^2}\right|^{2/\nu}\left[1-\mathrm{sign}\left(\frac{j\omega}{1-2j\omega\sigma_W^2}\right)\tan(\pi/\nu)\right]\right\} \quad (11)$$

$$\bar{C}(\lambda,R,\nu) = \frac{1}{R^2}\int_0^R\int_0^\infty \exp\left(-\frac{\sigma_n^2}{P_{\mathrm{u}}}(e^x-1)r_{\mathrm{f}}^\nu\right)\exp\left(-\frac{2\pi^2}{\nu}\csc\left(\frac{2\pi}{\nu}\right)\lambda\left(\frac{P_{\mathrm{i}}}{P_{\mathrm{u}}}(e^x-1)\right)^{2/\nu}r_{\mathrm{f}}^2\right)dx\,2r_{\mathrm{f}}dr_{\mathrm{f}} \quad (13)$$

IV. Traffic Offload

In order to evaluate the trade-off between the energy consumption and the achievable traffic offload, we define the small cell aggregate offload capacity and aggregate offload throughput which reflect the traffic that can be accommodated by the SAPs in a macrocell and also account for the sensing probability, the sensing time, and the sensing performance. We consider a saturated resource model, intending that each user always has a non-empty queue of data to be transmitted. The small cell capacity assumes adaptive modulation while the small cell throughput assumes a fixed transmission rate. Note that an exact analysis of the aggregate offload capacity and throughput requires an exact distribution of the area of the small cells which constitute a multiplicatively weighted Voronoi tessellation. The area distribution of a Voronoi tessellation is an open research problem for which an approximation has been proposed in [37]. Yet, in order to present a tractable analysis, we consider a distance based association policy with respect to the small cells. This relaxation of the original problem yields a unified framework that allows us to obtain both the detection performance and aggregate offload capacity and throughput.

A. Aggregate Offload Capacity

The aggregate capacity that can be offloaded per macrocell is given by the typical user uplink capacity in an SAP multiplied with the number of loaded and active SAPs within the macrocell coverage. Assuming OFDMA or TDMA, the typical user uplink capacity in an SAP equals the sum-capacity of N users sharing the same resource block. The expected number of SAPs per macrocell is given by $\lambda_{\mathrm{s}}/\lambda_{\mathrm{m}}$ [29]. We assume a distance based access policy with respect to the SAPs, where access can be granted when the mobile user is within the coverage R of the SAP. For this access policy, the probability that an SAP has at least one active user within the SAP coverage can be found by the complement of the null probability of a Poisson r.v. in (1) and is given by $p_{\mathrm{l}} = 1-\exp(-p_{\mathrm{u}}\lambda_{\mathrm{u}}\pi R^2)$. Let $N_{\mathrm{s}}^{(l)} = p_{\mathrm{l}}\lambda_{\mathrm{s}}/\lambda_{\mathrm{m}}$ be the expected number of SAPs in a macrocell with active users, then we define the capacity that can be offloaded from an MBS that accounts for the sensing procedure as follows:

$$\xi_c(\tau_{\mathrm{s}}) = N_{\mathrm{s}}^{(l)}p_{\mathrm{s}}\mathbb{P}_{\mathrm{d}}\frac{T-\tau_{\mathrm{s}}}{T}\bar{C}(\lambda,R,\nu) \quad (12)$$

where $\bar{C} = \mathbb{E}[\ln(1+\eta)]$ is the average channel capacity in uplink for a typical UE[7] and η is the signal-to-interference-and-noise ratio (SINR). The aggregate offload capacity is a function of the densities of MBSs, SAPs, and mobile users, where λ_{u} affects the offload capacity by changing the number of loaded small cells.[8] When the SoI and all the interfering signals are affected by Rayleigh fading, we can derive the average channel capacity in the next theorem as a special case of [38].

Theorem 2: A typical user is uniformly distributed over the coverage of the SAP, i.e. a circular area with radius R, while the interfering nodes are spatially scattered over the two-dimensional plane $\mathbb{R}^2$ according to a homogeneous PPP. The average channel capacity in the uplink of a typical user within the coverage of the associated SAP for a Rayleigh fading channel is given by (13) where P_{u} and P_{i} are the transmission power of the UE and of each interferer.

Proof: See Appendix B. □

Using Theorem 2, we formulate the following corollary for a special case.

Corollary 1: For $\nu = 4$, the average channel capacity of a typical user can be expressed as

$$\bar{C}(\lambda,R,4) = \int_0^\infty \frac{1}{2R^2}\sqrt{\frac{\pi}{b(x)}}\exp\left(\frac{a^2(x)}{4b(x)}\right) \times\left[\mathrm{erfc}\left(\frac{a(x)}{2\sqrt{b(x)}}\right)-\mathrm{erfc}\left(\frac{a(x)+2b(x)R^2}{2\sqrt{b(x)}}\right)\right]dx \quad (14)$$

where $a(x) = (\pi^2/2)\lambda\sqrt{(e^x-1)P_i/P_{\mathrm{u}}}$ and $b(x) = (\sigma_n^2/P_{\mathrm{u}})(e^x-1)$.

Proof: The proof of the corollary follows straightforwardly from [27] with some simple mathematical manipulations. □

The expression of the average channel capacity when $\nu = 4$ can be bounded using the bounds of the Q function $\exp(-x^2/2)/\sqrt{\pi}(x/\sqrt{2}+\sqrt{x^2/2+2}) < Q(x) < \exp(-x^2/2)/\sqrt{\pi}(x/\sqrt{2}+\sqrt{x^2/2+8/\pi})$.

B. Aggregate Offload Throughput

Assuming a constant transmission rate, the throughput that the small cell tier can accommodate and that accounts for the

[7]Note that we consider $X_{\mathrm{i},l}$ complex Gaussian and the interferers quasi-static.

[8]Note that we assume here that the coverage areas of different SAPs do not overlap, which is realistic considering a reduction of the coverage range with increasing small cell density.

$$\mathbb{P}_{\rm s}(\eta_t) = \frac{1}{R^2}\int_0^{R^2} \exp\left(-\frac{\sigma_n^2}{P_{\rm u}}\eta_t x^{\nu/2}\right) \exp\left(-\frac{2\pi^2}{\nu}\lambda\left(\frac{P_i\eta_t}{P_{\rm u}}\right)^{2/\nu}\csc\left(\frac{2\pi}{\nu}\right)x\right) dx \tag{16}$$

sensing strategy can be expressed as

$$\xi_t(\tau_{\rm s},\eta_t) = N_{\rm s}^{(l)} p_{\rm s}\mathbb{P}_{\rm d}\frac{T-\tau_{\rm s}}{T}\rho \tag{15}$$

where $\rho = \ln(1+\eta_t)\mathbb{P}_{\rm s}(\eta_t)$ is the throughput in uplink for a typical UE, η_t is the target SINR, and where the success probability is defined as $\mathbb{P}_{\rm s}(\eta_t) = \mathbb{P}[\eta > \eta_t]$.

Theorem 3: The success probability for a typical user in the coverage of an SAP and in the presence of network interference is given by (16).

Proof: See Appendix C. □

For the interference limited case, (16) becomes

$$\mathbb{P}_{\rm s}(\eta_t) = \frac{\exp(-\vartheta R^2)-1}{\vartheta} \tag{17}$$

where $\vartheta = \pi\lambda(2\pi/\nu)\csc(2\pi/\nu)(P_i\eta_t/P_{\rm u})^{2/\nu}$. For the special case of $\nu = 4$, we formulate the following corollary.

Corollary 2: For $\nu = 4$, the success probability of a typical user can be expressed as

$$\mathbb{P}_{\rm s}(\eta_t) = \frac{1}{2R^2}\sqrt{\frac{\pi}{d}}\exp\left(\frac{c^2}{4d}\right) \times\left[\operatorname{erfc}\left(\frac{c}{2\sqrt{d}}\right) - \operatorname{erfc}\left(\frac{c+2dR^2}{2\sqrt{d}}\right)\right] \tag{18}$$

where $c = \frac{\pi^2}{2}\lambda\csc\left(\frac{\pi}{2}\right)(\eta_t P_i/P_{\rm u})^{1/2}$ and $d = \sigma_n^2\eta_t/P_{\rm u}$.

Proof: Similar to proof in [27]. □

V. Traffic Offload versus Energy Consumption Trade-Off

In this section, we show how the framework developed in Sections III and IV can be useful for the design of energy efficient small cell networks by means of several optimization problems.

A. Optimization of energy consumption constrained by traffic offload

In the following, we first investigate the energy minimization with regard to the sensing time, and then optimize the energy consumption with respect to sensing time and sensing probability.

1) Optimization of sensing time: In this problem, the objective of the system design is to offload the traffic whenever there is an active user within the coverage of an SAP. Therefore, a constraint on $\mathbb{P}_{\rm d}$ is imposed and the problem can be formulated as

$$\begin{aligned}\min_{\tau_{\rm s}} \quad & E_{\rm tot} \\ \text{s.t.} \quad & \mathbb{P}_{\rm d}(\tau_{\rm s},\zeta) \geq \mathbb{P}_{\rm d}^*\end{aligned} \tag{19}$$

where $0 \leq \tau_{\rm s} \leq T$ and $\mathbb{P}_{\rm d}^*$ is the target probability of detection. For a given sensing time, a threshold ζ^* can be chosen as to satisfy the constraint $\mathbb{P}_{\rm d}(\tau_{\rm s},\zeta^*) = \mathbb{P}_{\rm d}^*$. Let $E_2(\mathbb{P}_{\rm d},\tau_{\rm s})$ and $E_3(\mathbb{P}_{\rm fa},\tau_{\rm s})$ denote the second and the third term of $E_{\rm tot}$ in (2), respectively. If we select a detection threshold $\zeta' < \zeta^*$ such that $\mathbb{P}_{\rm d}(\tau_{\rm s},\zeta') > \mathbb{P}_{\rm d}(\tau_{\rm s},\zeta^*)$ and $\mathbb{P}_{\rm fa}(\tau_{\rm s},\zeta') > \mathbb{P}_{\rm fa}(\tau_{\rm s},\zeta^*)$, then we also have $E_2(\mathbb{P}_{\rm d}(\tau_{\rm s},\zeta'),\tau_{\rm s}) > E_2(\mathbb{P}_{\rm d}(\tau_{\rm s},\zeta^*),\tau_{\rm s})$ and $E_3(\mathbb{P}_{\rm fa}(\tau_{\rm s},\zeta'),\tau_{\rm s}) > E_3(\mathbb{P}_{\rm fa}(\tau_{\rm s},\zeta^*),\tau_{\rm s})$. Therefore, the optimal solution is achieved under the equality constraint and the optimization problem can be reformulated as

$$\begin{aligned}\min_{\tau_{\rm s}} \quad & \lambda_{\rm s}/\lambda_{\rm m}[\Xi_c T + p_{\rm s}\Xi_{\rm s}\tau_{\rm s} + p_{\rm UE}p_{\rm s}\mathbb{P}_{\rm d}^*\Xi_t(T-\tau_{\rm s}) \\ & + (1-p_{\rm UE})p_{\rm s}\mathbb{P}_{\rm fa}(\tau_{\rm s},\zeta^*)\Xi_t(T-\tau_{\rm s})].\end{aligned} \tag{20}$$

For the special case of a user with fixed position and using the Gaussian approximation for the decision variable, the threshold value corresponding with $\mathbb{P}_{\rm d}^*$ is given by [32]

$$\zeta^* = \sigma_n^2(1+\eta)[1+\mathcal{Q}^{-1}(\mathbb{P}_{\rm d}^*)\sqrt{2/(\tau_{\rm s}f_{\rm s})}] \tag{21}$$

and $\mathbb{P}_{\rm fa}$ under the constraint of $\mathbb{P}_{\rm d}$ is given by

$$\mathcal{Q}\left(\frac{(1+\eta)[1+\mathcal{Q}^{-1}(\mathbb{P}_{\rm d}^*)\sqrt{2/(\tau_{\rm s}f_{\rm s})}]-1}{\sqrt{2/(\tau_{\rm s}f_{\rm s})}}\right). \tag{22}$$

Under this scenario, we formulate the following proposition.

Proposition 1: For a user with a fixed position and using the Gaussian approximation, the optimization problem as defined in (20) has a unique optimal solution $\tau_{\rm s}^*$.

Proof: See Appendix D □

2) Joint optimization of sensing time and sensing probability: Since it is energetically inefficient to sense continuously, to reduce idle listening we optimize the energy consumption with respect to $p_{\rm s}$ and $\tau_{\rm s}$ subject to constraints on ξ_c and $\mathbb{P}_{\rm d}$. The optimization problem can be formulated as

$$\begin{aligned}\min_{p_{\rm s},\tau_{\rm s}} \quad & E_{\rm tot} \\ \text{s.t.} \quad & \xi_c \geq \xi_c^*, \quad \mathbb{P}_{\rm d} \geq \mathbb{P}_{\rm d}^*\end{aligned} \tag{23}$$

which can be solved applying a two-step approach. For every value of $\tau_{\rm s} \in [0,T]$, the optimal sensing probability can be calculated reformulating the optimization problem as follows:

$$\begin{aligned}\min_{p_{\rm s}} \quad & E_{\rm tot} \\ \text{s.t.} \quad & \xi_c \geq \xi_c^*, \quad \mathbb{P}_{\rm d} \geq \mathbb{P}_{\rm d}^*.\end{aligned} \tag{24}$$

For a fix value of $\tau_{\rm s}$, we follow the argumentation of Section V-A to conclude that the optimal sensing probability can be found under the equality constraint. The optimal sensing probability is given by

$$p_{\rm s}^* = \frac{\xi_c^*}{N_{\rm s}^{(l)}\mathbb{P}_{\rm d}^*\frac{T-\tau_{\rm s}}{T}\bar{C}}. \tag{25}$$

To present a tractable analysis, we consider a user at a fixed distance from the SAP and apply the Gaussian approximation for the decision variable. The minimal energy consumption can be found by inserting (25) into (2). With $\mathbb{P}_{\rm d} = \mathbb{P}_{\rm d}^*$, $\mathbb{P}_{\rm fa} = \mathcal{Q}((\zeta^*-\sigma_n^2)/(\sqrt{2/(\tau_{\rm s}f_{\rm s})}\sigma_n^2))$, and $\zeta^* =$

$\mathcal{Q}^{-1}(\mathbb{P}^*_{\rm d})\sqrt{2/(\tau_{\rm s}f_{\rm s})}\sigma_n^2(1+\eta)+\sigma_n^2(1+\eta)$, (23) can be rewritten as

$$\min_{\tau_{\rm s}}\mathcal{K}(\tau_{\rm s})=\min_{\tau_{\rm s}}\quad\frac{\xi^*T}{N_{\rm s}^{(l)}\mathbb{P}^*_{\rm d}(T-\tau_{\rm s})\bar{C}}\Xi_{\rm s}\tau_{\rm s}+\frac{\xi^*T\Xi_t}{N_{\rm s}^{(l)}\mathbb{P}^*_{\rm d}\bar{C}}(p_{\rm UE}\mathbb{P}^*_{\rm d}+(1-p_{\rm UE})\mathbb{P}_{\rm fa}(\tau_{\rm s},\zeta^*)) \quad (26)$$

where $\mathbb{P}_{\rm fa}(\tau_{\rm s},\zeta^*)=\mathcal{Q}\left(\mathcal{Q}^{-1}(\mathbb{P}^*_{\rm d})(1+\eta)+\eta\sqrt{\tau_{\rm s}f_{\rm s}/2}\right)$. Since $\mathcal{K}(\tau_{\rm s})$ is differentiable on $[0,T]$, and $\mathcal{K}'(\tau_{\rm s})$ is increasing on $[0,T]$, $\mathcal{K}(\tau_{\rm s})$ is convex and there exists an optimal $\tau_{\rm s}^*$ for (26). For the limits of the sensing time interval, the first derivative of $\mathcal{K}$ is given by

$$\lim_{\tau_{\rm s}\to T}\mathcal{K}'(\tau_{\rm s})=\infty$$
$$\lim_{\tau_{\rm s}\to 0}\mathcal{K}'(\tau_{\rm s})=\frac{\xi^*\Xi_{\rm s}}{\mathbb{P}^*_{\rm d}\bar{C}}+\frac{\xi^*T\Xi_t}{\mathbb{P}^*_{\rm d}\bar{C}}(1-p_{\rm UE})\mathbb{P}'_{\rm fa}(\tau_{\rm s},\zeta^*) \quad (27)$$

where the last expression is negative if $\mathbb{P}'_{\rm fa}(0,\zeta^*)<-\Xi_{\rm s}/(\Xi_tT(1-p_{\rm UE}))$. Under this condition, the optimal sensing time can be found in the range $[0,T]$ by applying the bisection algorithm with tolerable sensing time error ϵ. The two-step optimization is illustrated in the following algorithm.

Algorithm 1 Joint optimization of the sensing time and sensing probability

```
Initialise τ_min ← 0,   τ_max ← T
while τ_max − τ_min > ε do
  τ_s ← (τ_min + τ_max)/2
  p*_s ← ξ*T/(P*_d(T − τ_s)C̄)
  if ∂E_tot(p*_s, τ_s)/∂τ_s < 0 then
    τ_min ← τ_s
  else
    τ_max ← τ_s
  end if
end while
```

B. Optimization of QoS under energy constraint

The system designer can decide to limit the energy consumption of a small cell. In this scenario, the optimization problem can be cast as

$$\max_{\tau_{\rm s}}\quad\xi_c(\tau_{\rm s})\quad\text{s.t.}\quad\mathbb{P}_{\rm fa}\le\mathbb{P}^*_{\rm fa}. \quad (28)$$

Following a similar reasoning as in Section V-A, we can show that the optimal solution can be found under the equality constraint. If we consider network interference, the detection threshold ζ can be found numerically using (9) and (11). In the case when we apply the Gaussian approximation for the decision variable, the threshold satisfying the constraint is given by $\zeta^*=\sigma_n^2(1+\sqrt{2/(\tau_{\rm s}f_{\rm s})}\mathcal{Q}^{-1}(\mathbb{P}^*_{\rm fa}))$. The optimization problem can now be reformulated as

$$\max_{\tau_{\rm s}}\quad\mathcal{Q}\left(\frac{\zeta^*-\sigma_n^2(1+\eta)}{\sqrt{2/(\tau_{\rm s}f_{\rm s})}\sigma_n^2(1+\eta)}\right)(T-\tau_{\rm s}). \quad (29)$$

With a change of variable $(\zeta^*-\sigma_n^2(1+\eta))/(\sqrt{2/(\tau_{\rm s}f_{\rm s})}\sigma_n^2(1+\eta))\to u$, it can be shown that there exists an optimal sensing time that yields the optimal capacity. Specifically, the optimal sensing time can be found as follows

$$\frac{\partial\xi_c(\tau_{\rm s})}{\partial\tau_{\rm s}}=N_{\rm s}^{(l)}p_{\rm s}\bar{C}\left[-\mathcal{Q}(u)+(T-\tau_{\rm s})\frac{e^{-u^2/2}}{\sqrt{2\pi}}\frac{du}{d\tau_{\rm s}}\right]=0 \quad (30)$$

where the optimal solution can be found numerically.

VI. SAP Performance Limits

In the former section, we illustrated how the proposed framework can be used to design energy efficient SAPs. In this section, we focus on the limits of the energy detector and obtain an expression of the $\mathbb{P}_{\rm fa}$ decay rate as a function of the aggregate network interference. As such, in the context of green communications, this analysis confines a region of interferer densities where the cognitive SAP can be used advantageously in order to reduce the network wide energy consumption.

A. Interference wall

In [32], [39], environment-dependent uncertainties are shown to be the cause of the so-called SNR wall, below which the detector is not robust regardless the sensing time. Noise uncertainty caused by the noise estimation has been discussed in [40]. An SAP with a UE within its coverage finds itself in a high-SNR environment, and therefore, the SNR-wall due to noise estimation is not relevant in this scenario. However, another source of uncertainty is the network interference. In the following, we derive an expression of the noise uncertainty due to the network interference.

1) Unbounded path-loss model: Under $\mathcal{H}_0$, the decision variable can be written as

$$V_{\rm ED}=\frac{1}{N}\sum_{k=1}^{N}(i[k]+n[k])^2. \quad (31)$$

As discussed in Appendix A, the network interference can be decomposed as $i[k]=\sqrt{U}G$, where U is a skewed stable distribution and G follows a normal distribution. Therefore, the received signal under $\mathcal{H}_0$ conditioned on U can be expressed as a normal r.v. $r[k]_{|\mathcal{H}_0,U}\sim\mathcal{N}(0,\sigma_n^2+2\gamma^{\nu/2}U)$. With γ defined as in (5), the variance of $r[k]_{|\mathcal{H}_0,U}$ can be written as $\sigma^2_{\rm tot}=\sigma_n^2+2\gamma^{\nu/2}U=\sigma^2_{\rm n}(1+2\eta_i(\pi C^{-1}_{4/\nu}\mathbb{E}[|h_lX^{\rm i}_{l,p}|^{4/\nu}])^{\nu/2}\lambda^{\nu/2}U)$, such that η_i is the interference-to-noise ratio (INR). Let $G=2\eta_i(\pi C^{-1}_{4/\nu}\mathbb{E}[|h_lX^{\rm i}_{l,p}|^{4/\nu}])^{\nu/2}U$, then the total variance takes values in the interval $\sigma^2_{\rm tot}\in[\sigma^2_{\rm n},\sigma^2_{\rm n}(1+\lambda^{\nu/2}G)]$ since the skewed stable distribution U only takes positive values. For high values of the sensing time, the central limit theorem can be applied and $\mathbb{P}_{\rm d}$ and $\mathbb{P}_{\rm fa}$ can be found in terms of Q-functions. In order to be robust with respect to the network interference, we get

$$\mathbb{P}_{\rm fa}=\mathcal{Q}\left(\frac{\zeta-(1+\lambda^{\nu/2}G)\sigma^2_{\rm n}}{\sqrt{2/N}(1+\lambda^{\nu/2}G)\sigma^2_{\rm n}}\right)$$
$$\mathbb{P}_{\rm d}=\mathcal{Q}\left(\frac{\zeta-(1+\text{SNR})\sigma^2_{\rm n}}{\sqrt{2/N}(1+\text{SNR})\sigma^2_{\rm n}}\right). \quad (32)$$

$$\mathcal{I} = \frac{2}{\nu/2-1}(d_{\min}^{2-\nu} - d_{\max}^{2-\nu}) \left(\frac{(\alpha-3)(\alpha-2)(d_{\min}^{2-\nu} - d_{\max}^{2-\nu})(\nu-1)}{(d_{\min}^{2-2\nu} - d_{\max}^{2-2\nu})(\nu/2-1)P_i\sigma_h^2} \right)^{\frac{2-\alpha}{2}+\frac{1}{2}(\alpha-2)} \eta_i \pi \sigma_h^2. \quad (36)$$

We define the sample complexity N^* as the sensing time needed to obtain the target $\mathbb{P}_{\rm d}$ and $\mathbb{P}_{\rm fa}$. Eliminating ζ from the equations in (32) and solving to N, the sample complexity can be written as

$$N^* = \frac{2(\mathcal{Q}^{-1}(\mathbb{P}_{\rm fa})(1+G\lambda^2) - \mathcal{Q}^{-1}(\mathbb{P}_{\rm d})(1+\text{SNR}))^2}{(\text{SNR} - G\lambda^{\nu/2})^2}. \quad (33)$$

It follows that as $\lambda \to (\text{SNR}/G)^{2/\nu}$, we have $N^* \to \infty$. In other words, a target $\mathbb{P}_{\rm fa}$ and $\mathbb{P}_{\rm d}$ cannot be attained within a finite sensing time for some interfering node density approaching $(\text{SNR}/G)^{2/\nu}$. We call this limit the interference wall $\lambda_{\rm wall,s}$ and note that $\lambda_{\rm wall,s}$ is a function of the SNR, INR, the power path loss exponent, and the fading. However, to calculate G, a percentile of the distribution has to be selected that corresponds to a worst case, due to the heavy tails of the stable distribution.

2) Bounded path-loss model: The heuristic approximation based on the stable distribution is computationally intensive and sensitive to the selection of the percentile. In order to find a solution with higher accuracy, we consider that the interferers are located in the annulus $\mathcal{A}$, defined by the radii $d_{\min}$ and $d_{\max}$. Under such conditions, it can be shown that $i[k]$ in (31) follows a truncated stable distribution [41]

$$i[k] \sim S_t(\gamma', \alpha = 4/\nu, g) \quad (34)$$

where α corresponds to the characteristic exponent of the stable distribution, γ' corresponds to the dispersion, and g reflects the decaying of the tail of the truncated stable distribution. The coefficients γ' and g can be determined by the method of the cumulants, by imposing the equality of the second and fourth cumulant of the truncated stable distribution with the respective cumulants of the network interference. Applying the approach of Section VI-A1, we further approximate the interference by a Gaussian r.v., such that the received signal follows a normal distribution $r[k]_{|\mathcal{H}_0} \sim \mathcal{N}(0, \sigma_n^2 + \sigma_i^2)$, where σ_i^2 represents the second order moment of the truncated stable distribution

$$\sigma_i^2 = \mathbb{E}[i^2[k]] = \frac{\partial^2 M_{\rm i}(t,\lambda)}{\partial t^2}|_{t=0} = \sigma_n^2 \mathcal{I}\lambda \quad (35)$$

where $M_{\rm i}(t,\lambda)$ is the moment generating function (MGF) of the truncated stable distribution. After some manipulations, $\mathcal{I}$ can be expressed as (36). Note that the variance of the network interference is linear in the interferer density λ and the parameter $\mathcal{I} = f(d_{\min}, d_{\max}, \nu, \eta_i, \sigma_h^2)$. For $\nu = 4$, the parameter $\mathcal{I}$ further simplifies to $2(d_{\min}^{-2} - d_{\max}^{-2})P_i\pi\sigma_h^2$. Eliminating ζ from the expressions of $\mathbb{P}_{\rm d}$ and $\mathbb{P}_{\rm fa}$, the sample complexity can now be expressed as

$$N^* = \frac{2(\mathcal{Q}^{-1}(\mathbb{P}_{\rm fa})(1+\mathcal{I}\lambda) - \mathcal{Q}^{-1}(\mathbb{P}_{\rm d})(1+\text{SNR}))^2}{(\text{SNR} - \mathcal{I}\lambda)^2} \quad (37)$$

and the interference wall is given by $\lambda_{\rm wall,t} = \text{SNR}/\mathcal{I}$.

B. False alarm decay

To express the relationship between energy consumption and interfering node density, we determine how fast $\mathbb{P}_{\rm fa}$ converges to its target value. As such, we provide a tool to evaluate how increasing the sensing time affects the energy efficiency. A direct method to obtain the PDF of $V_{\rm ED}$ as a function of the sensing time is cumbersome[9]. Instead, we will use tools from large deviations theory to determine how fast the target $\mathbb{P}_{\rm fa}$ can be reached. According to the Cramer theorem, we have for interference-limited networks

$$\mathbb{P}_{\rm fa}(\zeta) = \mathbb{P}[1/N \sum_N i^2[k] > \zeta] \leq e^{-NI(\zeta)} \quad (38)$$

which decays exponentially with the sensing time and the decay rate is determined by the rate function $I(x)$. In order to have finite moments, we model the aggregate interference power $I_\Omega = \sum i^2[k]$ according to a truncated stable distribution. The CF of the truncated stable distribution is given by [42]

$$\psi_{I_\Omega}(j\omega) = \exp\left(\gamma'\Gamma(-\alpha')\left[(g-j\omega)^{\alpha'} - g^{\alpha'}\right]\right) \quad (39)$$

where α' is chosen equal to the characteristic exponent of the stable distribution in the unbounded path loss model. The parameters of the truncated stable distribution can be found using the method of the cumulants. From (39), the cumulants of the truncated stable distribution can be expressed as

$$\begin{aligned} \kappa_I(n) &= \frac{1}{j^n}\frac{d^n}{d\omega^n}\ln\psi_{I_\Omega}(j\omega)\Big|_{\omega=0} \\ &= (-1)^n\gamma'\Gamma(-\alpha')g^{\alpha'-n}\Pi_{i=0}^{n-1}(\alpha'-i). \end{aligned} \quad (40)$$

Building on Cambell's theorem [41], the cumulants of the aggregate interference can be expressed as

$$\kappa(n) = P_{\rm i}^n \frac{2\pi\lambda}{2-n\nu}(d_{\max}^{2-n\nu} - d_{\min}^{2-n\nu})\mu_{h^2}(n). \quad (41)$$

Using (40) and (41), the parameters γ' and g can be written as a function of the first two cumulants as follows

$$\begin{aligned} \gamma' &= \frac{-\kappa(1)}{\Gamma(-\alpha')\alpha'\left(\frac{\kappa(1)(1-\alpha')}{\kappa(2)}\right)^{\alpha'-1}} \\ g &= \frac{\kappa(1)(1-\alpha')}{\kappa(2)}. \end{aligned} \quad (42)$$

Since $i^2[k]$ are assumed to be i.i.d., the Cramer theorem can be applied and we can express the rate function as the Legendre-Fenchel transform of the logarithmic MGF

$$I(x) = \sup_\theta \left(\theta x - \gamma'\Gamma(-\alpha')[(g-\theta)^{\alpha'} - g^{\alpha'}]\right). \quad (43)$$

For $\theta < g$, let the first derivative be equal to zero and solving to θ for $\nu = 4$, we have

$$\theta = g - \left(\frac{-\gamma'\Gamma(-\alpha')}{2x}\right)^2. \quad (44)$$

[9]Note that we expressed the CF of $V_{\rm ED}$ in Section III-B

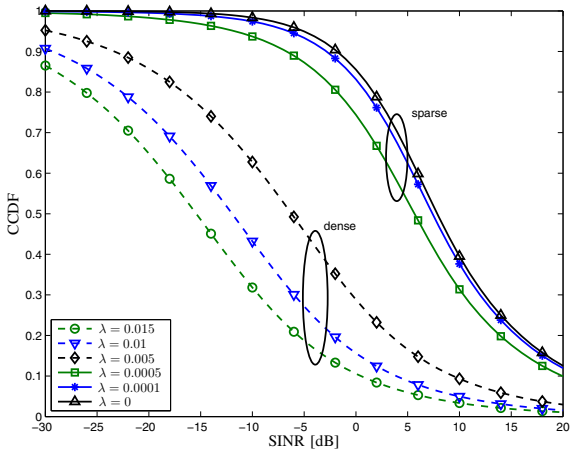

Fig. 3. The success probability in the presence of sparse and dense interferers.

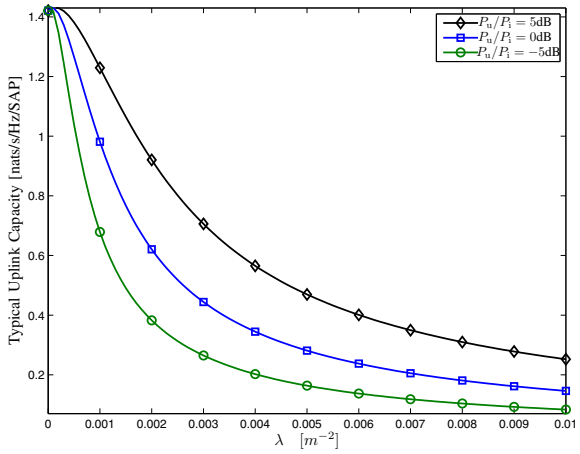

Fig. 4. The average channel capacity corrected by the detection probability for different values of the power ratio between the SoI and the interferers.

Substituting θ in (43), the expression of the rate function is given by

$$I(x) = gx + \sqrt{g}\gamma'\Gamma(-\alpha) + \frac{(\gamma'\Gamma(-\alpha'))^2}{4x}. \qquad (45)$$

VII. Numerical Results

In this section, we present some numerical results that provide insight into the trade-off between energy consumption and traffic offload of the SAPs within a MBS Voronoi cell.

A. Traffic offload

Figure 3 depicts the success probability for a typical user within the coverage of an SAP. With the interferers distributed according to a PPP, this figure illustrates that the success probability decreases drastically with increasing interfering node density. Figure 4 shows $\mathbb{P}_{\mathrm{d}}\bar{C}$ (the uplink capacity of a typical user in the SAP coverage corrected for the detection probability) as a function of the interferer density. The figure illustrates the combined effect of the increasing detection performance and the decreasing average channel capacity with λ.

B. SAP energy efficiency

Since this work focuses on the trade-off between the energy consumption and the aggregate offload throughput and capacity, it is meaningful to analyze how the energy consumption depends on the interferer density. In the following numerical examples, we consider that SNR = 3 dB defined for the UE at the edge of the SAP coverage $R = 20$, while the INR = 10 dB defined at a distance of 1 meter (far-field assumption). We consider the densities of MBSs, SAPs, and users to be $\lambda_{\mathrm{m}} = 10^{-6}$ m^{-2} , $\lambda_{\mathrm{s}} = 10^{-5}$ m^{-2}, and $\lambda_{\mathrm{u}} = 10^{-4}$ m^{-2}. From (2), we observe that the power consumption consists of three components Ξ_c, Ξ_{s}, and Ξ_t, which we assume to be constant and given by $\Xi_c = 6W$, $\Xi_{\mathrm{s}} = 4W$, and $\Xi_t = 5W$ [43]. Unless otherwise specified, we set the probabilities $p_{\mathrm{I}} = 0.1$, $p_{\mathrm{s}} = 1$, and $p_{\mathrm{UE}} = 0.1$. Furthermore, we let the frame length $T = 400/f_{\mathrm{s}}$ and the maximum duty cycle (DC) is 25 %.

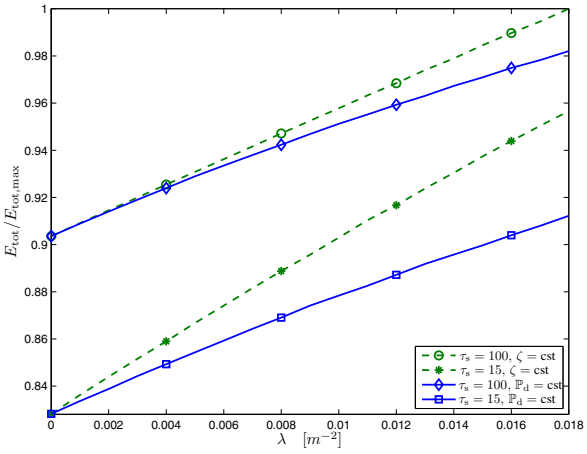

Fig. 5. Total energy consumption for different values of the sensing time and with fix or variable detection threshold value.

Figure 5 shows the total energy consumption considering a constant target $\mathbb{P}_{\mathrm{d}}$ and a constant threshold, respectively. We observe that for all scenarios the energy consumption grows with increasing interfering node density. This can be ascribed to the fact that the energy consumption is linear in $\mathbb{P}_{\mathrm{d}}$ and $\mathbb{P}_{\mathrm{fa}}$. As more energy is provided to the ED with increasing interferer density, $\mathbb{P}_{\mathrm{d}}$ and $\mathbb{P}_{\mathrm{fa}}$ increase for the constant threshold scenario. In this numerical example, $p_{\mathrm{UE}} = 0.1$ and therefore, the increase of energy consumption is dominated by $\mathbb{P}_{\mathrm{fa}}$. If information is available about the interference environment, the threshold can be altered such that $\mathbb{P}_{\mathrm{d}} = \mathbb{P}_{\mathrm{d}}^{*}$. Raising the threshold with the interferer density, moderates the increase of $\mathbb{P}_{\mathrm{fa}}$ and the energy consumption, which is reflected in the figure. This means that the knowledge of the interference environment allows to improve the energy efficiency of small cell networks.

Figure 6 illustrates the effect of the SAP coverage range and the interferer node density on the energy consumption. The energy consumption increases with almost 50 % when R varies from 15 to 50 m. The sensing time is fixed to $N = 15$

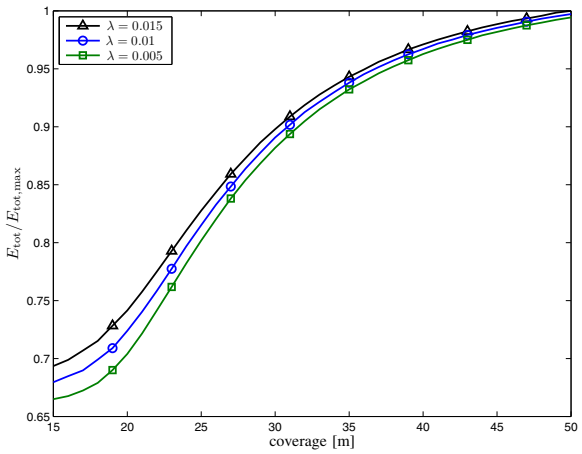

Fig. 6. Total energy consumption for different values of the interferer density.

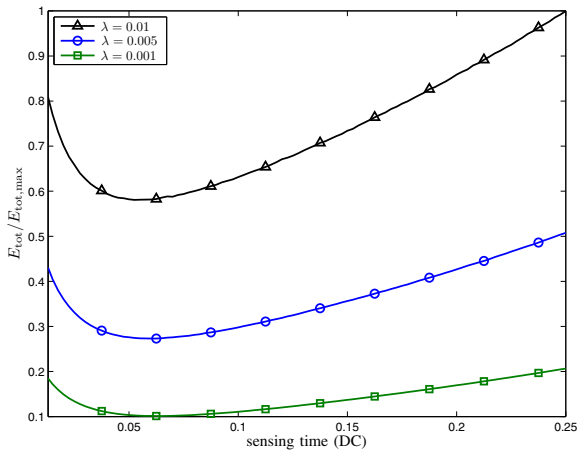

Fig. 7. E_{tot} for different values of the interferer density and with $p_{\mathrm{UE}} = 0.1$. The optimization is performed subject to $\mathbb{P}_{\mathrm{d}}^{*} = 0.9$ and $\xi_c^{*} = 0.5$ nats/s/Hz/macrocell.

samples and $\mathbb{P}_{\mathrm{d}} = \mathbb{P}_{\mathrm{d}}^{*} = 0.9$ for all values of the coverage. To satisfy the constraint on $\mathbb{P}_{\mathrm{d}}$, the detection threshold decreases for a larger coverage, and as a consequence $\mathbb{P}_{\mathrm{fa}}$ increases. This is reflected in the total energy consumption. From the numerical results presented in Fig. 6, we can conclude that the energy consumption is affected considerably by changing the SAP coverage due to the strong relation between the user detection performance and the coverage range.

In Section V-A2, we defined an optimization problem that minimizes the energy consumption subject to constraints on both the traffic offload and the detection probability. Figure 7 depicts the objective function (23) of the energy consumption optimization problem for different interferer densities. We ascertain the convexity of the energy consumption of all SAPs belonging to a macrocell Voronoi cell subject to constraints on $\mathbb{P}_{\mathrm{d}}$ and ξ_c. The initial decrease of the energy consumption is due to the decrease of $\mathbb{P}_{\mathrm{fa}}$ with the sensing time until $\mathbb{P}_{\mathrm{fa}}$ reaches a stationary value. Any further increase of the energy consumption is related to the sensing energy accruing with the sensing time. Furthermore, this example reveals that for increasing interferer density, the optimal sensing time decreases, which can be ascribed to a higher stationary $\mathbb{P}_{\mathrm{fa}}$ with increasing λ. The impact of λ on the optimal sensing time is however negligible. This result highlights that the proposed framework can be used to find the optimal sensing time and sensing probability. Moreover, we observe that the energy consumption can be improved considerably and the energy consumption gain by joint optimization of τ_{s} and p_{s} increases with larger interferer density.

To elucidate the trade-off between the energy consumption and the traffic offload, we define the energy efficiency as $\varsigma = \xi_c / E_{\mathrm{tot}}$. Figure 8 shows the effect of the sensing time and the interferer density on the energy efficiency. We observe that there exists an optimal value of the sensing time balancing the two opposing requirements. With respect to the optimization of the energy consumption subject to a constraint on $\mathbb{P}_{\mathrm{d}}$, this figure shows that with increasing interferer density the optimal sensing time shifts to smaller values. This effect is related to the linear decrease of the traffic offload with increasing sensing time, as can be verified in (12) or (15).

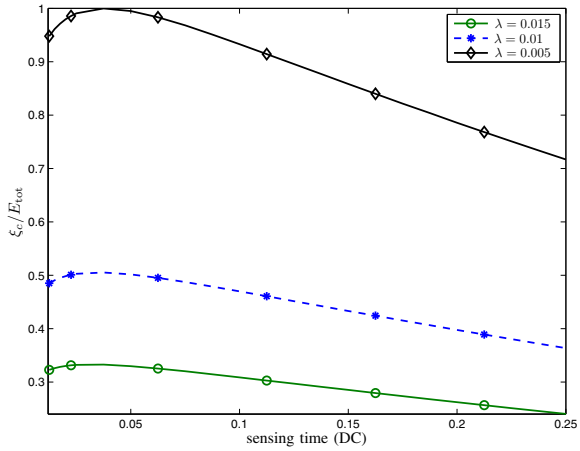

Fig. 8. Energy efficiency for different values of λ as a function of the sensing duty cycle.

Defining the load of a typical base station (SAP or MBS) as the number of active users within the coverage, we notice that the small cell load is related to the density of the active users and the small cell coverage. Owing to the major coverage differences between the tiers, the load of a typical SAP and MBS differ considerably such that the aggregate offload capacity depends on λ_{m}, λ_{s}, and λ_{u}. Figure 9 illustrates how the energy consumption and the traffic offload of the SAPs within a macrocell vary as a function of λ_{u} and how they relate. The numerical results illustrate the impact of the quality of the cognitive capabilities on both the energy consumption and traffic offload. In this scenario, we assume λ_{u} to vary as $10^{-6} < \lambda_{\mathrm{u}} < 10^{-3}$ and that SIR $= 0$dB. For sensing DC = 0.05, the energy efficiency ς is clearly superior than for higher values of the duty cycle. In case of perfect sensing and low values of the load, the energy consumption is lower than the curves with realistic detection performance due to $\mathbb{P}_{\mathrm{fa}} = 0$, and this effect diminishes with increasing load.

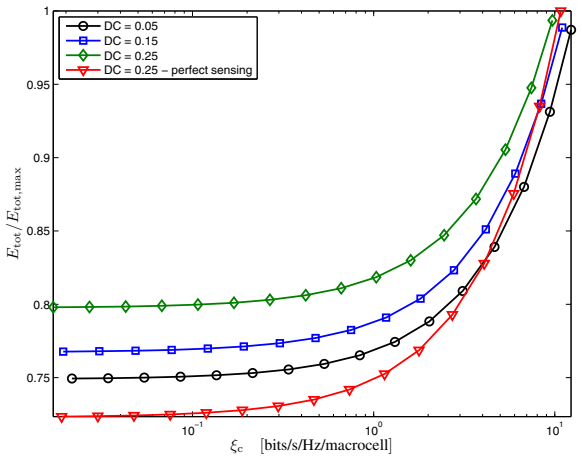

Fig. 9. Energy consumption for different values of the sensing time and for the ideal case of perfect sensing as a function of the load.

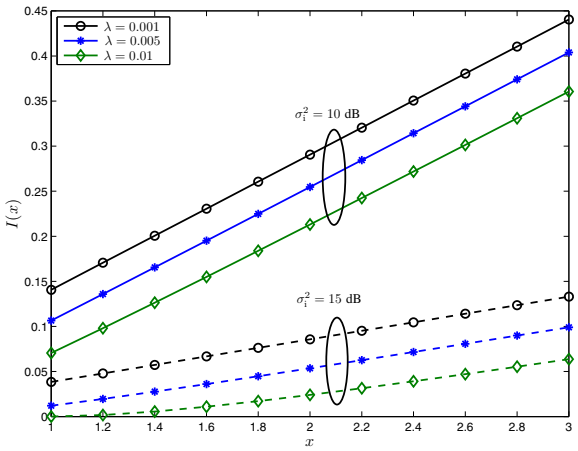

Fig. 11. The rate function is given for different values of the interference power and density.

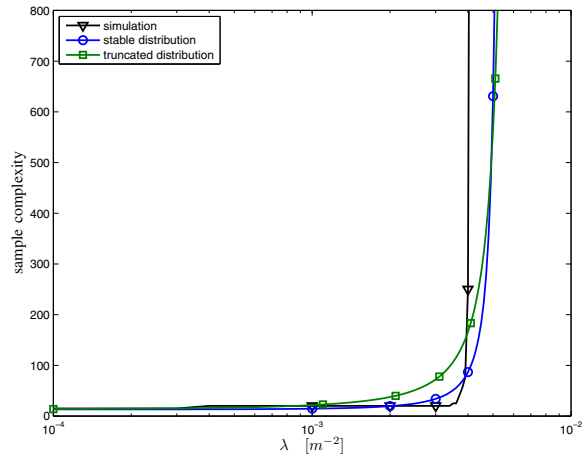

Fig. 10. The interference wall using the approximation with the 87 percentile of the stable distribution, using the truncated stable distribution and using numerical simulations for $\mathbb{P}_{\mathrm{fa}}^{*} = 0.1$ and $\mathbb{P}_{\mathrm{d}}^{*} = 0.9$, SNR = 3 dB and INR = 20 dB.

C. Performance limits

Figure 10 shows the sample complexity to satisfy a target $\mathbb{P}_{\mathrm{fa}}$ and $\mathbb{P}_{\mathrm{d}}$ for increasing interferer density. This figure illustrates the fundamental limit of the interfering node density under which the SAP can robustly detect the macrocell user presence. Beyond the interference wall, the noise uncertainty becomes too big to distinguish between SoI or noise. The curves are drawn using the 87 percentile of the stable distribution, the truncated stable distribution and numerical simulations. For $d_{\min} = 1$ and $d_{\max} = 100$, the approaches with the stable and the truncated stable distribution are in good agreement and correspond well with the numerical simulation. Figure 11 shows the $\mathbb{P}_{\mathrm{fa}}$ decay rate as expressed in (45) as a function of the threshold x for different values of the interference power and the interferer density. It can be observed that with increasing density and interference power the rate function decreases. Thus, the rate function can reveal more insight into the effect of λ and P_{i} on the SAP power consumption and reflects the achievable energy efficiency.

VIII. Conclusions

In this paper, we proposed an analytical framework that allows to analyze the trade-off between the energy consumption and the traffic offload of cognitive SAPs located in an MBS Voronoi cell. In particular, we defined the detection performance of an energy detector for a typical user, as well as the aggregate capacity and throughput that can be offloaded from an MBS. The model accounts for channel fading, aggregate network interference, bursty activity, network topology, and load. The proposed model allows to quantify the effect of critical system parameters such as the interferer density and the SAP coverage on the detection performance, the aggregate offload capacity and throughput, and the total energy consumption. Numerical results reveal that the knowledge of the interference environment can lead to a substantial reduction of the SAP energy consumption. We defined several optimization problems and showed that the proposed framework can be used both for the design of the optimal sensing time and sensing probability, as for the evaluation of the energy efficiency with respect to network topology and load. Further, fundamental limits of the detection robustness are defined by introducing the interference wall and the speed of convergence of $\mathbb{P}_{\mathrm{fa}}$. In conclusion, the framework can be used for the energy efficient design and operation of cognitive SAPs in heterogeneous networks. Possible future directions to extend this work are to consider the combined energy consumption of multiple tiers, include constraints on the user quality of service, and compare the effectiveness of the distributed sleep mode scheme with strategies such as random sleeping or centralized sleep mode schemes exploiting user location awareness.

IX. Acknowledgment

This work was partly supported by the SRG ISTD 2012037, CAS Fellowship for Young International Scientists Grant 2011Y2GA02, SUTD-MIT International Design Centre under

Grant IDSF1200106OH, the A*STAR Research Attachment Programme, and the European Commission Marie Curie International Outgoing Fellowship under Grant 2010-272923.

APPENDIX A
PROOF OF THEOREM 1

Proof: Let $S = s[k]/\sqrt{N}$, $I = i[k]/\sqrt{N}$ and $W = n[k]/\sqrt{N}$ with $\sigma_n^2/N = \sigma_W^2$, then the discrete decision statistic in (8) can be rewritten as

$$V_{\mathrm{ED}|\mathcal{H}_1} = \sum_{k=1}^{N} \Big(\underbrace{\frac{h}{r_{\mathrm{f}}^{\nu/2}} S[k] + I[k]}_{K} + W[k] \Big)^2.$$

Conditioning on K, V_{ED} follows a non-central chi-square distribution and therefore, the CF of V_{ED} is given by

$$\psi_{V_{\mathrm{ED}}|\mathcal{H}_1,K}(j\omega) = \frac{1}{\left(1-2j\omega\sigma_W^2\right)^{N/2}} \exp\left(\frac{j\omega N K^2}{1-2j\omega\sigma_W^2}\right). \tag{46}$$

Since the network interference follows a symmetric stable distribution, the decomposition property can be applied and the interference can be represented as $I = \sqrt{U}G$, with $U \sim \mathcal{S}(2/\nu, 1, \cos(\frac{\pi}{\nu}))$ and $G \sim \mathcal{N}(0, 2\gamma^{\nu/2}/N)$. If we assume that the SoI has a normal distribution, then K^2 in (46) stands for the power of a normally distributed r.v. with variance $h^2 P_{\mathrm{u}}/(r_{\mathrm{f}}^{\nu} N) + 2\gamma^{\nu/2} U/N$. Let $V = 2\gamma^{\nu/2}U$, then we can write

$$\psi_{V_{\mathrm{ED}}|\mathcal{H}_1,h,r_{\mathrm{f}},V}(j\omega) = \frac{1}{\left(1-2j\omega\sigma_W^2\right)^{N/2}} \exp\left(\frac{j\omega N(h^2 P_{\mathrm{u}}/(r_{\mathrm{f}}^{\nu} N) + V/N)}{1-2j\omega\sigma_W^2}\right).$$

The exponential can be expanded as the product of two exponentials. Further deconditioning on h and V, we get

$$\psi_{V_{\mathrm{ED}}|\mathcal{H}_1,r_{\mathrm{f}}}(j\omega) = \frac{1}{\left(1-2j\omega\sigma_W^2\right)^{N/2-1}} \times \frac{1}{1-j\omega(P_{\mathrm{u}}/(2r_{\mathrm{f}}^{\nu}) + \sigma_W^2)} \psi_V\left(\frac{j\omega}{1-2j\omega\sigma_W^2}\right).$$

Using the scaling property of a stable random variable, the CF of the decision variable can be written as

$$\begin{aligned}\psi_{V_{\mathrm{ED}}|\mathcal{H}_1,r_{\mathrm{f}}}(j\omega) =& \frac{1}{\left(1-2j\omega\sigma_W^2\right)^{N/2-1}} \\ &\times \frac{1}{1-j\omega(P_{\mathrm{u}}/(2r_{\mathrm{f}}^{\nu}) + \sigma_W^2)} \\ &\times \exp\left\{-2^{2/\nu}\gamma\cos(\pi/\nu)\left|\frac{j\omega}{1-2j\omega\sigma_W^2}\right|^{2/\nu}\right. \\ &\left.\times\left[1-\mathrm{sign}\left(\frac{j\omega}{1-2j\omega\sigma_W^2}\right)\tan(\pi/\nu)\right]\right\}.\end{aligned}$$

We take the expectation with respect to r_{f} bearing in mind that the UE is within the range $[0, R]$ and that the probability density function (PDF) of r_{f} is given by $f_X(r_{\mathrm{f}}) = 2r_{\mathrm{f}}/R^2$. Solving the expectation, the proof is concluded. □

APPENDIX B
PROOF OF THEOREM 2

Proof: The average capacity of a typical user can be written as

$$\bar{C} = \mathbb{E}_{r_{\mathrm{f}},\phi,h}[\ln(1+\eta)]$$

where the expectation is taken over the distance r_{f} between the UE and the SAP, over the spatial PPP ϕ of the interferers and over the fading distribution h. For a positive r.v. X, $\mathbb{E}[X] = \int_0^\infty 1 - F_X(x)dx$ with $F_X(x)$ the cumulative distribution function. Following the approach of [27], the average throughput can be expressed as

$$\bar{C} = \int_0^R \int_0^\infty \exp\left(-\frac{\sigma_n^2}{P_{\mathrm{u}}}(e^x-1)r_{\mathrm{f}}^{\nu}\right) \times \mathcal{L}_I\left(\frac{e^x-1}{P_{\mathrm{u}}} r_{\mathrm{f}}^{\nu}\right) dx \frac{2r_{\mathrm{f}}}{R^2} dr_{\mathrm{f}} \tag{47}$$

where $\mathcal{L}_I(s)$ is the Laplace transform of the network interference I. Applying the probability generating functional of the PPP and assuming that the interfering signal is affected by Rayleigh fading, we can write

$$\mathcal{L}_I\left(\frac{e^x-1}{P_{\mathrm{u}}} r_{\mathrm{f}}^{\nu}\right) = \exp\left[-2\pi\lambda \int_0^\infty \left(1 - \frac{1}{1+\frac{P_i}{P_{\mathrm{u}}}(e^x-1)(r_{\mathrm{f}}/u)^{\nu}}\right) u du\right]$$

which by a change of variables can further be simplified to

$$\mathcal{L}_I\left(\frac{e^x-1}{P_{\mathrm{u}}} r_{\mathrm{f}}^{\nu}\right) = \exp\left(-\frac{2\pi^2}{\nu}\csc\left(\frac{2\pi}{\nu}\right)\lambda\left(\frac{P_i}{P_{\mathrm{u}}}\right)^{2/\nu}(e^x-1)^{2/\nu} r_{\mathrm{f}}^2\right). \tag{48}$$

Inserting (48) in (47), the proof is concluded. □

APPENDIX C
PROOF OF THEOREM 3

Proof: The success probability for a typical user in the coverage of the SAP is given by

$$\mathbb{P}_{\mathrm{s}}(\eta_t) = \mathbb{E}_{r_{\mathrm{f}},\phi,h}\left\{\mathbb{P}\left[\frac{h^2 P_{\mathrm{u}} r_{\mathrm{f}}^{-\nu}}{\sigma_n^2 + I} > \eta_t\right]\right\}.$$

For a typical user uniformly distributed over the coverage of the SAP and considering Rayleigh fading, we can write

$$\mathbb{P}_{\mathrm{s}}(\eta_t) = \int_0^R \exp\left(-\frac{r_{\mathrm{f}}^{\nu}\eta_t\sigma_n^2}{P_{\mathrm{u}}}\right)\mathbb{E}_\phi\left[\exp\left(-\frac{r_{\mathrm{f}}^{\nu}\eta_t I}{P_{\mathrm{u}}}\right)\right]\frac{2r_{\mathrm{f}}}{R^2}dr_{\mathrm{f}}$$

where $\mathbb{E}_\phi\left[\exp\left(-r_{\mathrm{f}}^{\nu}\eta_t I/P_{\mathrm{u}}\right)\right] = \mathcal{L}_I(r_{\mathrm{f}}^{\nu}\eta_t/P_{\mathrm{u}})$. Evaluating the Laplace transform of the network interference (48) at $r_{\mathrm{f}}^{\nu}\eta_t/P_{\mathrm{u}}$, the proof is concluded. □

APPENDIX D
PROOF OF PROPOSITION 1

Proof: Let $\mathcal{G}(\tau_\mathrm{s})$ be the objective function in (20). If $\mathcal{G}(\tau_\mathrm{s})$ is differentiable over $[0,T]$, then $\mathcal{G}(\tau_\mathrm{s})$ is convex iff $\mathcal{G}'(\tau_\mathrm{s})$ is increasing over the considered interval. We write the derivative of $\mathcal{G}(\tau_\mathrm{s})$ with respect to τ_s as

$$\mathcal{G}'(\tau_\mathrm{s}) = \lambda_\mathrm{s}/\lambda_\mathrm{m}[p_\mathrm{s}\Xi_\mathrm{s} - p_\mathrm{u}p_\mathrm{s}\mathbb{P}_\mathrm{d}^*\Xi_t - (1-p_\mathrm{u})p_\mathrm{s}\mathbb{P}_\mathrm{fa}(\zeta^*,\tau_\mathrm{s})\Xi_t + (1-p_\mathrm{u})p_\mathrm{s}\Xi_t(T-\tau_\mathrm{s})\mathbb{P}'_\mathrm{fa}(\zeta^*,\tau_\mathrm{s})]. \quad (49)$$

For $\zeta^* > \sigma_n^2$, $\mathbb{P}_\mathrm{fa}$ is positive and decreasing with τ_s, while $\mathbb{P}'_\mathrm{fa}$ is negative and increasing with τ_s. Therefore, the third and fourth term in (49) are increasing over $[0,T]$. Since the first two terms in the expression of $\mathcal{G}'(\tau_\mathrm{s})$ are constant, this concludes the proof. □

REFERENCES

[1] T. Q. S. Quek, G. de la Roche, I. Guvenc, and M. Kountouris, *Small Cell Networks: Deployment, PHY Techniques, and Resource Allocation*. Cambridge University Press, 2013.

[2] D. Lopez-Perez, I. Guvenc, G. de la Roche, M. Kountouris, T. Q. S. Quek, and J. Zhang, "Enhanced intercell interference coordination challenges in heterogeneous networks," *IEEE Wireless Commun. Mag.*, vol. 18, no. 3, pp. 22-30, Jun. 2011.

[3] J. G. Andrews, H. Claussen, M. Dohler, S. Rangan, and M. C. Reed, "Femtocells: past, present, and future," *IEEE J. Sel. Areas Commun.*, vol. 30, no. 3, pp. 497–508, Apr. 2012.

[4] H. Bogucka and A. Conti, "Degrees of freedom for energy savings in practical adaptive wireless systems," *IEEE Commun. Mag.*, vol. 49, no. 6, pp. 38–45, Jun. 2011.

[5] Y. S. Soh, T. Q. S. Quek, M. Kountouris, and H. Shin, "Energy efficient heterogeneous cellular networks," *IEEE J. Sel. Areas Commun.*, vol. 31, no. 5, pp. 840–850, May 2013.

[6] Y. Chen, S. Zhang, S. Xu, and G. Li, "Fundamental trade-offs on green wireless networks," *IEEE Commun. Mag.*, vol. 49, no. 6, pp. 30–37, Jun. 2011.

[7] W. C. Cheung, T. Q. S. Quek, and M. Kountouris, "Throughput optimization, spectrum allocation, and access control in two-tier femtocell networks," *IEEE J. Sel. Areas Commun.*, vol. 30, no. 3, pp. 561–574, Apr. 2012.

[8] A.-H. Tsai, L.-C. Wang, J.-H. Huang, and R.-B. Hwang, "High-capacity OFDMA femtocells by directional antennas and location awareness," *IEEE Systems J.*, vol. 6, no. 2, pp. 329–340, Jun. 2012.

[9] S. Wu, C. Chen, and M. Chen, "Collaborative wakeup in clustered ad hoc networks," *IEEE J. Sel. Areas Commun.*, vol. 29, no. 8, pp. 1585–1594, Sep. 2011.

[10] A. Azad, S. Alouf, E. Altman, V. Borkar, and G. Paschos, "Optimal control of sleep periods for wireless terminals," *IEEE J. Sel. Areas Commun.*, vol. 29, no. 8, pp. 1605–1617, Sep. 2011.

[11] W. Guo and T. O'Farrell, "Green cellular network: deployment solutions, sensitivity and tradeoffs," in *Proc. 2011 Wireless Advanced*, pp. 42–47.

[12] I. Ashraf, F. Boccardi, and L. Ho, "Sleep mode techniques for small cell deployments," *IEEE Commun. Mag.*, vol. 49, no. 8, pp. 72–79, Aug. 2011.

[13] I. Haratcherev, M. Fiorito, and C. Balageas, "Low-power sleep mode and out-of-band wake-up for indoor access points," in *Proc. 2009 IEEE Global Telecomm. Conf.*, pp. 1–6.

[14] L. Saker, S. E. Elayoubi, R. Combes, and T. Chahed, "Optimal control of wake up mechanisms of femtocells in heterogeneous networks," *IEEE J. Sel. Areas Commun.*, vol. 30, no. 3, pp. 664–672, Apr. 2012.

[15] H. El Sawy and E. Hossain, "Two-tier hetnets with cognitive femtocells: downlink performance modeling and analysis in a multi-channel environment," *IEEE Trans. Mobile Comput.*, 2013, accepted for publication.

[16] Y. C. Liang, Y. Zeng, E. C. Y. Peh, and A. T. Hoang, "Sensing-throughput tradeoff for cognitive radio networks," *IEEE Trans. Wireless Commun.*, vol. 7, no. 4, pp. 1326–1337, Apr. 2008.

[17] F. Moghimi, A. Nasri, and R. Schober, "Adaptive L_p-norm spectrum sensing for cognitive radio networks," *IEEE Trans. Commun.*, vol. 59, no. 7, pp. 1934–1945, Jul. 2011.

[18] S. M. Cheng, W. C. Ao, and K. C. Chen, "Efficiency of a cognitive radio link with opportunistic interference mitigation," *IEEE Trans. Wireless Commun.*, vol. 10, no. 6, pp. 1715–1720, Jun. 2011.

[19] E. Axell, G. Leus, E. G. Larsson, and H. V. Poor, "Spectrum sensing for cognitive radio," *IEEE Signal Process. Mag.*, vol. 29, no. 3, pp. 101–116, May 2012.

[20] Q. Zhao and B. M. Sadler, "A survey of dynamic spectrum access," *IEEE Signal Process. Mag.*, vol. 24, no. 3, pp. 79–89, May 2007.

[21] K. C. Chen and R. Prasad, *Cognitive Radio Networks*. Wiley, 2009.

[22] T. V. Nguyen, H. Shin, T. Q. S. Quek, and M. Z. Win, "Sensing and probing cardinalities for active cognitive radios," *IEEE Trans. Signal Process.*, vol. 60, no. 4, pp. 1833–1848, Apr. 2012.

[23] L. Saker, S. E. Elayoubi, L. Rong, and T. Chahed, "Capacity and energy efficiency of picocell deployment in LTE-A networks," in *Proc. 2011 IEEE Int. Veh. Technol. Conf.*, pp. 1–5.

[24] S. M. Cheng, S. Y. Lien, F. S. Chu, and K. C. Chen, "On exploiting cognitive radio to mitigate interference in macro/femto heterogeneous networks," *IEEE Wireless Commun. Mag.*, vol. 18, no. 3, pp. 40–47, Jun. 2011.

[25] C. H. M. de Lima, M. Bennis, and M. Latva-aho, "Coordination mechanisms for self-organizing femtocells in two-tier coexistence scenarios," *IEEE Trans. Wireless Commun.*, vol. 11, no. 6, pp. 2212–2223, Jun. 2012.

[26] Y. S. Soh, T. Q. S. Quek, M. Kountouris, and G. Caire, "Cognitive hybrid division duplex for two-tier femtocell networks," *IEEE Trans. Wireless Commun.*, 2013, accepted for publication.

[27] J. G. Andrews, F. Baccelli, and R. K. Ganti, "A tractable approach to coverage and rate in cellular networks," *IEEE Trans. Commun.*, vol. 59, no. 11, pp. 3122–3134, Nov. 2011.

[28] B. Blaszczyszyn, M. K. Karray, and H.-P. Keeler, "Using Poisson processes to model lattice cellular networks," in *Proc. 2013 IEEE Joint Conf. of the IEEE Computer and Commun. Societies*, pp. 797–805.

[29] S. G. Foss and S. A. Zuyev, "On a Voronoi aggregative process related to a bivariate Poisson process," *Advances in Applied Probability*, pp. 965–981, 1996.

[30] T. Yucek and H. Arslan, "A survey of spectrum sensing algorithms for cognitive radio applications," *IEEE Commun. Surveys Tuts.*, vol. 11, no. 1, pp. 116–130, First Quarter 2009.

[31] D. Bhargavi and C. R. Murthy, "Performance comparison of energy, matched-filter and cyclostationarity-based spectrum sensing," in *Proc. 2010 IEEE Workshop on Signal Proc. Advances in Wireless Commun.*, pp. 1–5.

[32] R. Tandra and A. Sahai, "SNR walls for signal detection," *IEEE J. Sel. Topics Signal Process.*, vol. 2, no. 1, pp. 4–17, Feb. 2008.

[33] J. F. C. Kingman, *Poisson Processes*. Oxford University Press, 1993.

[34] I. Ashraf, L. Ho, and H. Claussen, "Improving energy efficiency of femtocell base stations via user activity detection," in *Proc. 2010 IEEE Wireless Commun. and Networking Conf.*

[35] M. Z. Win, P. C. Pinto, and L. A. Shepp, "A mathematical theory of network interference and its applications," *Proc. IEEE*, vol. 97, no. 2, pp. 205–230, Feb. 2009.

[36] P. C. Pinto and M. Z. Win, "Communication in a Poisson field of interferers—part I: interference distribution and error probability," *IEEE Trans. Wireless Commun.*, vol. 9, no. 7, pp. 2176–2186, Jul. 2010.

[37] J. S. Ferenc and Z. Néda, "On the size distribution of Poisson Voronoi cells," *Physica A: Statistical Mechanics and its Applications*, vol. 385, no. 2, pp. 518–526, Nov. 2007.

[38] T. D. Novlan, H. S. Dhillon, and J. G. Andrews, "Analytical modeling of uplink cellular networks," *IEEE Trans. Wireless Commun.*, 2013, accepted for publication.

[39] A. Sahai, S. M. Mishra, and R. Tandra, *Cognitive Radios: System Design Perspective*. Springer, 2009, ch. Spectrum Sensing: Fundamental Limits.

[40] A. Mariani, A. Giorgetti, and M. Chiani, "Effects of noise power estimation on energy detection for cognitive radio applications," *IEEE Trans. Commun.*, vol. 59, no. 12, pp. 3410–3420, Dec. 2011.

[41] A. Rabbachin, T. Q. S. Quek, H. Shin, and M. Z. Win, "Cognitive network interference," *IEEE J. Sel. Areas Commun.*, vol. 29, no. 2, pp. 480–493, Feb. 2011.

[42] A. Rabbachin, A. Conti, and M. Z. Win, "Intentional network interference for denial of wireless eavesdropping," in *Proc. 2011 IEEE Global Telecomm. Conf.*, pp. 4268–4273.

[43] G. Auer, V. Giannini, C. Desset, I. Godor, P. Skillermark, M. Olsson, M. Imran, D. Sabella, M. Gonzalez, O. Blume, and A. Fehske, "How much energy is needed to run a wireless network?" *IEEE Wireless Commun. Mag.*, vol. 18, no. 5, pp. 40–49, Oct. 2011.

Matthias Wildemeersch (S'09) received the M.S. degree in Elecromechanical Engineering from the University of Ghent (Belgium) in 2003. He is currently working towards the PhD degree in Electrical Engineering at the University of Twente (the Netherlands). From 2008 to 2011 he was at the Joint Research Centre of the European Commission, where he worked on the impact assessment of interference related to GNSS. Since 2012, he is with the Institute for Infocomm Research (Singapore) where his work broadly covers the analysis of heterogeneous networks. His research interests span various aspects of wireless communications and signal processing and focus on the application of probability theory and stochastic geometry to green communications, cognitive radio, and interference mitigation. He received the IEEE SPAWC 2013 Best Student Paper Award and is an awardee of the A*STAR Research Attachment Programme (2012-2013).

Tony Q. S. Quek (S'98-M'08-SM'12) received the B.E. and M.E. degrees in Electrical and Electronics Engineering from Tokyo Institute of Technology, Tokyo, Japan, in 1998 and 2000, respectively. At Massachusetts Institute of Technology (MIT), Cambridge, MA, he earned the Ph.D. in Electrical Engineering and Computer Science in Feb. 2008.

Currently, he is an Assistant Professor with the Information Systems Technology and Design Pillar at Singapore University of Technology and Design (SUTD). He is also a Scientist with the Institute for Infocomm Research. His main research interests are the application of mathematical, optimization, and statistical theories to communication, networking, signal processing, information theoretic, and resource allocation problems. Specific current research topics include cooperative networks, heterogeneous networks, green communications, smart grid, wireless security, compressed sensing, and cognitive radio.

Dr. Quek has been actively involved in organizing and chairing sessions, and has served as a member of the Technical Program Committee (TPC) in a number of international conferences. He served as the Cognitive Radio & Cooperative Communications Track Chair for the IEEE VTC in spring 2011, the Wireless Communications Symposium Chair for the IEEE Globecom in 2011, and the Communication Theory Symposium Chair for the IEEE WCSP in 2013. He is currently an Editor for the IEEE TRANSACTIONS ON COMMUNICATIONS and the IEEE WIRELESS COMMUNICATIONS LETTERS. He was Guest Editor for the *IEEE Communications Magazine* (Special Issue on Heterogeneous and Small Cell Networks) in 2013. He received the Singapore Government Scholarship in 1993, Tokyu Foundation Fellowship in 1998, and the A*STAR National Science Scholarship in 2002. He was honored with the 2008 Philip Yeo Prize for Outstanding Achievement in Research, the IEEE Globecom 2010 Best Paper Award, the 2011 JSPS Invited Fellow for Research in Japan, the CAS Fellowship for Young International Scientists in 2011, the 2012 IEEE William R. Bennett Prize, and the IEEE SPAWC 2013 Best Student Paper Award.

Cornelis H. Slump received the M.Sc. degree in Electrical Engineering from Delft University of Technology, the Netherlands in 1979. In 1984 he obtained his Ph.D. in physics from the University of Groningen, the Netherlands. From 1983 to 1989 he was employed at Philips Medical Systems in Best as head of a predevelopment group on image quality and cardiovascular image processing. In 1989 he joined the Network Theory group from the University of Twente, Enschede, the Netherlands. His main research interest is in detection and estimation, interference reduction and pattern analysis as a part of digital signal processing. In June 1999 he was appointed as a full professor and heads the Signals and Systems group.

Alberto Rabbachin (S'03-M'07) received the Master Degree in telecommunications engineering from the University of Bologna (Italy) and the Ph.D. degree in electrical engineering from the University of Oulu (Finland), in 2001 and 2008, respectively. In 2011, he joined the Laboratory for information and decision systems (LIDS) at the Massachusetts Institute of Technology (MIT), where he is currently a Marie Curie Fellow. He was a postdoctoral researcher with the Institute for the Protection and Security of the Citizen of the European Commission Joint Research Center from 2008 to 2011. His research interests involve communication theory and stochastic geometry applied to real-problems in wireless networks including network secrecy, cognitive radio, ultrawide-band transceiver design, network synchronization, ranging techniques, and interference exploitation. Dr. Rabbachin is an Editor of the IEEE COMMUNICATION LETTERS and served as symposium and workshop chair in various IEEE conferences. He received the IEEE Communications Society William R. Bennett Prize in the Field of Communications Networking (2012), the IEEE Globecom best paper award (2010), the European Commission JRC best young scientist award (2010), and the Nokia Fellowship (2005, 2006). He is a recipient of the International Outgoing Marie Curie Fellowship (2011-2014).